2021-09-15

Inorganic nitrogen and phosphorus in Western European aerosol and the significance of dry deposition flux into stratified shelf waters

White, C

http://hdl.handle.net/10026.1/17348

1 **Inorganic nitrogen and phosphorus in Western European aerosol and the**

2 **significance of dry deposition flux into stratified shelf waters**

3

4 **Caroline White[1], Simon J. Ussher[1], Mark F. Fitzsimons[1], Sov Atkinson[1], E. Malcolm S.**

5 **Woodward[2], Mingxi Yang[2], Thomas G. Bell[2]**

6 **[1] Biogeochemistry Research Centre, School of Geography, Earth and Environmental Science,**

7 **University of Plymouth, Drake Circus, Plymouth, PL4 8AA, UK**

8 **[2] Plymouth Marine Laboratory, Prospect Place, Plymouth, PL1 3DH, UK**

9

10 ABSTRACT

11 Dry deposition of nitrogen (N) and phosphorus (P) from the aerosol phase represents a potential

12 source of nutrients to marine surface waters. To investigate the significance of this deposition

13 pathway, aerosol samples were collected from Penlee Point Atmospheric Observatory in SW England,

14 UK, over a 6-month period (February to July 2015) covering the spring bloom. Samples were analysed

15 for nitrate, ammonium and phosphate and the dry deposition flux of these nutrients calculated to

16 assess its potential impact on primary production in nearby surface seawater. Aerosol-derived N and

17 P deposition fluxes ranged from 2.7 - 620 μmol N m^{-2} d^{-1} and 0.16 - 1.6 μmol P m^{-2} d^{-1}, respectively.

18 Air mass back trajectory analysis indicated that the highest N fluxes were associated with polluted

19 European air masses, highlighting a significant anthropogenic influence on N-content of aerosols. The

20 N:P ratios of aerosol fluxes and water column concentrations indicated that P deposition was unlikely

21 to be biologically significant in the region. In contrast, aerosol deposition was a significant episodic

22 source of new N to marine phytoplankton after the onset of water column stratification. Carbon

23 fixation estimates indicated that the maximum proportion of new primary production sustained by

24 aerosol-N deposition was 22.4 %, a factor of ten higher than the study average. These data suggest

25　that enhanced N-deposition from polluted continental air masses could sustain pulses of surface

26　ocean biological productivity during periods of dissolved N depletion.

27

1. INTRODUCTION

29　Reactive nitrogen (N) and phosphorus (P) are vital macronutrients in surface seawater, fuelling

30　primary production by marine phytoplankton and the biological carbon pump (Elser *et al.*, 2007).

31　Anthropogenic activities in the last century have created new sources of reactive N and significantly

32　altered the global nitrogen cycle (Duce *et al.*, 2008; Galloway *et al.*, 2003; Martino *et al.*, 2014).

33　Emission model studies estimate a fourfold increase in inorganic nitrogen emissions since 1850 (Duce

34　*et al.*, 2008; Jickells *et al.*, 2017; Krishnamurthy *et al.*, 2009). The Redfield ratio of N to P uptake (16:1)

35　in phytoplankton means that small changes to the P pool can impact the N:P ratio if the system is close

36　to Redfield (Elser *et al.*, 2007).

37　Atmospheric reactive N is made up of inorganic oxidised forms (nitrate, NO_3^-, and nitrite, NO_2^-), and

38　the inorganic reduced form, ammonia/ammonium (NH_3/NH_4^+), as well as an organic N fraction (Hertel

39　*et al.*, 2012). Atmospheric reactive N in the aerosol phase can be transported long distances from

40　emission sources, potentially spanning continents and ocean basins. From the perspective of primary

41　production, approximately 70% of the surface ocean is N limited or N co-limited with P (Moore *et al.*,

42　2013). Atmospheric deposition can introduce significant pulses of reactive N to N-limited surface

43　waters (Kim *et al.*, 2014; Okin *et al.*, 2011; Owens *et al.*, 1992).

44　Anthropogenic emissions of oxidised N are primarily derived from N oxides from combustion

45　processes such as road transportation, shipping and industry (Hertel *et al.*, 2012; Okin *et al.*, 2011). A

46　large proportion of gas phase N oxides (NO_x) undergo atmospheric transformation to form nitric acid,

47　which displaces chloride on the surface of sea salt particles (typically coarse mode, >1 µm diameter)

48　in the marine boundary layer (Ottley & Harrison, 1992; Yeatman, Spokes & Jickells, 2001)**.** Emissions

49   of reduced N are predominately from agricultural sources, as well as from biomass burning (Hertel *et*

50   *al.*, 2012; Okin *et al.*, 2011)**.** Gas phase NH_3 is very soluble and readily protonates in the aqueous phase

51   of the aerosol to form the NH_4^+ ion. Nitric acid also reacts with NH_3 to form fine mode (<1 μm diameter)

52   ammonium nitrate aerosol (Yeatman, Spokes & Jickells, 2001)**.**

53   Jickells *et al.* (2017) estimated global inorganic nitrogen emissions as ca. 100 Tg N yr^{-1}. Reactive N

54   emission estimates for Europe were reported by Leip *et al.* (2011): NO_x emissions totalled 3.5 Tg N yr^{-1}

55   and were dominated by road transport (1.3 Tg N yr^{-1}) and combustion from industry (1.0 Tg N yr^{-1}).

56   Reduced N (NH_3/NH_4^+) emissions totalled 3.2 Tg N yr^{-1} and were dominated by agriculture at 3.0 Tg N

57   yr^{-1} (Leip *et al.*, 2011). Hence, the emission ratio of oxidised and reduced N species both in Europe and

58   globally is estimated to be approximately 1:1 even though the sources are not the same.

59   Phosphorus is mainly emitted to the atmosphere as aerosol (Myriokefalitakis *et al.*, 2016). The

60   principal sources include mineral dust (48 %), anthropogenic (14 %) and biogenic emissions (34 %;

61   from plants, animals and bacteria). Total P in the atmosphere predominately comprises insoluble

62   mineral dusts, orthophosphates, soluble and insoluble organic P (Myriokefalitakis *et al.*, 2016).

63   Orthophosphate (PO_4^{3-}) is the most common and bioavailable form of soluble P in the ocean (Björkman

64   & Karl, 2003; Mahowald *et al.*, 2008). Mahowald *et al.,* (2008) estimated that 0.74 Tg of PO_4^{3-} is

65   released to the atmosphere each year across the globe. These global estimates, which are derived

66   from a wealth of past measurements, e.g. Baker *et al.,* (2006; 2007; 2010; 2017), suggest that

67   anthropogenic activity has not significantly altered aerosol PO_4^{3-} concentrations. Based on the global

68   estimates for N and P emissions (Jickells *et al*., 2017; Mahowald *et al.*, 2008) the global atmospheric

69   N:P ratio is greater than 400, hence it can further be concluded that globally the aerosol phase is N

70   rich compared to P.

71   Atmospheric deposition can provide an important additional source of soluble N to marine surface

72   waters under certain conditions. Previous studies observed several significant N deposition events

73   from air masses originating from Europe and estimated that N deposition could support up to 30 % of

74 new daily primary production in the NE Atlantic Ocean (Spokes *et al.,* 2000; Spokes and Jickells, 2005).

75 In seasonally stratified waters during the spring/summer months, water column stratification can trap

76 nutrients within a limited depth range in the sunlit euphotic zone, which facilitates phytoplankton

77 growth but can also isolate them from remineralised nutrient sources at depth. Sustained biological

78 activity draws down available nutrients to the point where external inputs of N (e.g. from atmospheric

79 deposition) have the potential to be highly significant (Chester & Jickells, 2012; Spokes & Jickells, 2005;

80 Spokes *et al.*, 2000; Owens *et al.,* 1992). However, it must be noted that stratification within the water

81 column is a dynamic feature which varies in depth and can even be broken down by strong physical

82 processes (e.g. winds, currents). A complete breakdown in stratification allows nutrients trapped in

83 the deep shelf water to be mixed throughout the water column, thus resupplying the surface with

84 nutrients, including bioavailable N and P (Schmidt *et al*., 2020; Maier *et al*., 2012; Lentz *et al*., 2003).

85 Carbon flux and carbon fixation measurements in coastal and shelf regions, during seasons with active

86 primary production, have shown that wet and dry deposition of N can contribute 0.4 – 3.7 % of new

87 primary production (Park *et al*., 2019; Kocak, 2015; Singh *et al*., 2012). Even in regions of significant

88 wind driven upwelling such as the Californian coastline, atmospheric N-deposition is estimated to

89 account for up to 8 % of new productivity (Mackey *et al*., 2010). The largest impact of atmospheric N

90 deposition has been found in regions of high population density and air pollution. In the SE China

91 coastline, 5.6 – 19.4 % of new primary production is supported by N-deposition from nearby

92 anthropogenic sources during winter and summer seasons (Wang *et al*., 2019). These studies

93 demonstrate that increased inputs of reactive nitrogen to coastal regions from anthropogenic sources

94 will have significant impact on coastal marine primary production in the future, as predicted by several

95 global modelling studies (Duce *et al*., 2008; Baker *et al*., 2017).

96 The aim of this study was to integrate atmospheric aerosol and marine nutrient observations at a well-

97 studied coastal time-series site in order to estimate the impact of atmospheric reactive soluble N and

98 P deposition on seasonally stratified shelf waters. The study site is situated on the south-west coast

99   of England, UK, and uses atmospheric time-series data from Penlee Point Atmospheric Observatory

100   (PPAO) and seawater time-series data from the Western Channel Observatory (WCO). The data were

101   collected between February and July 2015, spanning the period of water column stratification and the

102   phytoplankton spring bloom.

2. METHODS

104   Atmospheric data were collected from the PPAO, situated on the Rame Head Peninsula on the western

105   edge of Plymouth Sound, Cornwall, UK (50°19.080 N, 4°11.350 W). The coastal site is exposed to a

106   number of distinct wind sectors/air masses, including the North Atlantic Ocean from the southwest,

107   and mainland Europe/ship emission within the English Channel from the east/southeast (Figure 1).

108   The PPAO was established in 2014 by Plymouth Marine Laboratory (PML) in collaboration with the

109   University of Plymouth and detail on the site characteristics is presented elsewhere (Yang *et al.,* 2019;

110   Yang *et al.*, 2016a; Yang *et al.*, 2016b). Gas phase carbon dioxide, methane, sulfur dioxide, ozone and

111   meteorological variables (wind speed, wind direction, relative humidity, atmospheric pressure and

112   rain rate) are continuously monitored. Aerosol samples were collected weekly and analysed at the

113   University of Plymouth (UoP) for inorganic nutrients.

114   Seawater samples and data were collected from L4, a long-term coastal monitoring buoy located 6 km

115   south of PPAO (50°15.00' N, 4°13.02' W). L4 is a key sampling station for the Western Channel

116   Observatory (WCO, http://www.westernchannelobservatory.org.uk). Continuous measurements at

117   the L4 buoy include PAR, sea surface temperature, salinity and chlorophyll. Routine weekly water

118   column samples are collected from L4 for nutrient concentrations (NO_2^-, NO_3^-, NH_4^+, PO_4^{3-}),

119   (Woodward & Harris, 2019), and are analysed in a shore-based laboratory by a SEAL Analytical

120   segmented flow autoanalyzer using colorimetric analysis techniques (Woodward & Rees, 2001).

121   Concurrent temperature and salinity profiles are collected weekly by CTD from the RV Plymouth

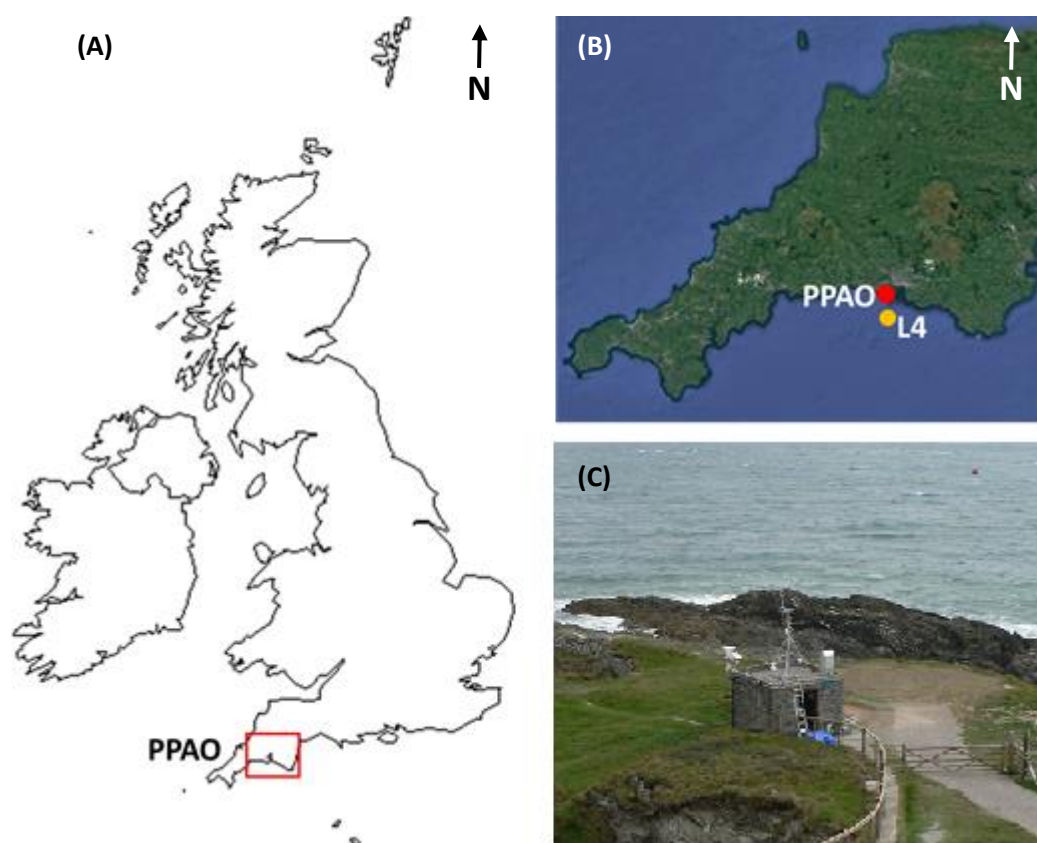122   Quest.

123

124

125

126

Figure 1: *(A) Location of study area. (B) Location of Penlee Point Atmospheric Observatory (PPAO) and*

of the Western Channel Observatory marine time series L4 station/buoy. (C) Site in Spring 2015 (photo

taken facing south). Aerosol samples were collected from a Hi-Vol sampler positioned on the SW corner

of the roof of the building.

Aerosol Sampling and Analysis

Particulate aerosol samples were collected onto acid-cleaned and combusted 8 x 10" (203 x 254 mm)

Whatman Quartz Microfiber Filters (QMA) using a Tisch Environmental (model TE-5170) high-volume

aerosol sampler (approximately 1 m^3 min^{-1} flow rate), which was calibrated in accordance with the

product handbook using a manometer once a month. Samples (n = 22) were collected weekly from 9th

February to 14th July 2015. Filters were pre-loaded into an aluminium filter cassette for sampling and

137 protected by an aluminium cover until sampling began. There was a sampling gap from 5th-26th March

138 due to a sampler malfunction. During the sampling days, air was filtered for either 24 hours (9th

139 February-9th April) or 12 hours (9th April-14th July). Filter samples were collected and sealed in zip-lock

140 bags, then transported in an insulated container for storage (-20 °C freezer) and analysis at the UoP

141 laboratory. Aerosol filters samples were prepared for analysis by subsampling into quarters and

142 submerging one subsample in 125 mL of high purity water (HPW; ≥ 18.2 MΩ cm) overnight to leach

143 the soluble N and P into solution (Cornell & Jickells, 1999). Leaching efficiency was assessed by

144 performing a second extraction on sub-samples. All analytes of secondary extractions were below the

145 limit of detection, confirming high efficiency of the initial single extraction.

146 Aerosol NO_2^-, NO_3^- and PO_4^{3-} were determined by spectrophotometric analysis based on Hansen and

147 Koroleff, (2007) and Gardolinski *et al.,* (2001), using a continuous flow, air-segmented nutrient auto

148 analyser (Skalar SAN[plus] series 1074). Instrumental precision was determined from the relative

149 standard deviation (RSD) of triplicate measurements. Mean RSD for NO_3^- + NO_2^- was 2.84 % (n = 22),

150 and for PO_4^- was 1.34 % (n = 22), which is consistent with inter-comparison studies involving the same

151 instrument (Birchill *et al.*, 2019). Concentrations of NO_2^- for aerosols are typically below detection

152 limits (approx. 0.1 nmol m^{-3}: Baker *et al.*, 2010; Lesworth, Baker & Jickells, 2010), so this small fraction

153 (< 4% maximum: 0.2% median) was combined with NO_3^- and reported as aerosol NO_3^-. Ammonium

154 (NH_4^+) was analysed by fluorimetry, using a Hitachi F-4500 fluorometer (see Holmes *et al.,* 1999). Air

155 concentrations were calculated by dividing the detected values by the total volume of air that had

156 passed through the filter.

157 **Dry Deposition Fluxes**

158 Dry deposition fluxes were calculated to investigate the importance of aerosol as a source of nutrients

159 to coastal waters (Spokes & Jickells, 2005). Here, fluxes are calculated as daily (24 h) inputs, hence the

160 airmass concentrations collected over a 12 h period have been interpolated as a constant 24 h

161   concentration. The deposition flux (Equation 1) is the product of the aerosol concentration (C) and the

162   deposition velocity (V_d):

163                              $$Flux = C\ V_d \qquad\qquad\qquad (1)$$

164   The deposition velocity is influenced by physical processes such as gravitational settling, impaction

165   and diffusion, which are constrained by particle size, wind speed and sea surface conditions (Duce *et*

166   *al.*, 1991). The deposition velocity is not well quantified (Baker *et al.,* 2010; Duce *et al.*, 1991) and

167   there is a large uncertainty on current estimates. We used a particle size-dependent V_d value: 2.0 cm

168   s^{-1} for coarse mode particles (diameter > 1 μm) and 0.1 cm s^{-1} for fine mode particles (diameter < 1

169   μm) (Duce *et al.*, 1991; Slinn & Slinn, 1980). These V_d values were chosen to enable comparison with

170   other studies (e.g. Spokes & Jickells, 2005; Yeatman *et al.*, 2001).

171   Samples collected from PPAO were not size-segregated, so it was necessary to estimate the relative

172   distribution of NO_3^-, NH_4^+ and PO_4^{3-} within the fine and coarse mode aerosol. PO_4^{3-} sources

173   predominantly generate larger sized (> 1 μm) aerosols, with the exception of combustion sources

174   which can either be greater or less than 1 μm (Myriokefalitakis *et al.*, 2016; Mahowald *et al*., 2008).

175   Combustion sources represent approximately 14 % of global aerosol PO_4^{3-} (Mahowald *et al*., 2008), so

176   we assume that all aerosol PO_4^{3-} was in the coarse mode and apply a deposition velocity of 2.0 cm s^{-1},

177   appropriate to >1μm particle sizes to calculate the deposition flux (Duce *et al.*, 1991). Defining size

178   distributions for NO_3^- and NH_4^+ is more challenging as previous studies have shown that coarse and

179   fine mode ratios of NO_3^- and NH_4^+ are highly dependent on source region (Bencs *et al.*, 2009; Spokes

180   & Jickells, 2005; Yeatman *et al.*, 2001). PPAO is situated between two well- established atmospheric

181   observatories, Mace Head, Galway (Ireland) and Weybourne, Norfolk (UK). Mace Head and

182   Weybourne are exposed to the same air mass sectors described at PPAO and size segregated NO_3^- and

183   NH_4^+ measurements have been made for these sectors (Spokes & Jickells, 2005; Yeatman *et al.*, 2001).

184   We used the Mace Head and Weybourne data (Table 1) to estimate the size distribution of NO_3^- and

185   NH$_4^+$ in the air masses encountered at PPAO for this study. The uncertainty related to this estimation

186   has been taken into account in any discussion of fluxes.

187   **Table 1:** Percentage medians (± range) of coarse mode (> 1µm) NO$_3^-$ and NH$_4^+$ found in aerosols from

188   source region extrapolated from Spokes & Jickells (2005) and Yeatman *et al* (2001).

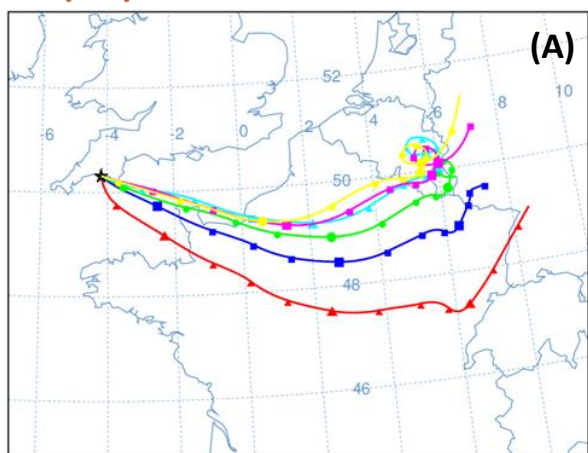| Source Region	> 1µm NH$_4^+$	> 1µm NO$_3^-$
N Atlantic Clean	18.5 % (± 17.5%)	70 % (± 21 %)
N Atlantic Mixed	20.5 % (± 5.5)	65 % (± 12 %)
Channel Mixed	36.5 % (± 0.5 %)	69 % (± 1 %)
Continental	43.5 % (± 1.5 %)	48.5 (± 8.5 %)

189

190   **Source Region Analysis**

191   Wind sectors have been defined previously for PPAO using the local wind direction (Yang *et al.*, 2016a).

192   In this study, we combined the local wind direction with air mass back trajectory analysis to categorise

193   the source region of each aerosol sample. Air mass back trajectories were calculated using the

194   National Oceanic and Atmospheric Administration (NOAA) HYbrid Single-Particle Lagrangian

195   Integrated Trajectory (HYSPLIT) model (http://ready.arl.noaa.gov/HYSPLIT.php). A back trajectory was

196   calculated every 6 hours while the aerosol sampler was running, resulting in 3 trajectories for 12 hour

197   samples and 6 trajectories for 24 hour samples. Trajectories were initiated at 20 m above ground level

198   and run backwards for 72 hours.
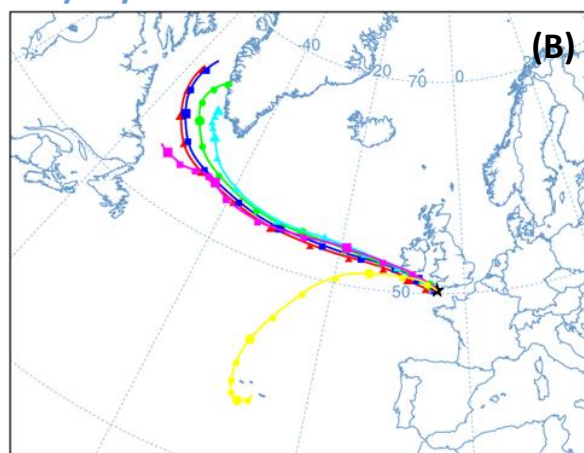
199   Each sample was classified into one of four air mass source regions using the local wind speed and

200   direction (Yang *et al.*, 2016a) and its HYSPLIT back trajectory. The four wind sectors are the

201   Continental, North Atlantic, Channel Mixed and N Atlantic Mixed (see examples in Figure 2). The

202   predominant wind direction at PPAO is from the West/South-West, and the North Atlantic Ocean is

203   the dominant influence on this air (North Atlantic). Air from the West and North-West often originates

over the North Atlantic, but has spent time over Ireland and rural parts of the UK prior to reaching the

PPAO (N Atlantic Mixed). Winds from the East/South-East have been influenced by ship emissions in

the English Channel and anthropogenic/terrestrial emissions from continental Europe (Continental).

During low wind speed events, the air tends to stagnate in the local area, picking up a mixture of ship

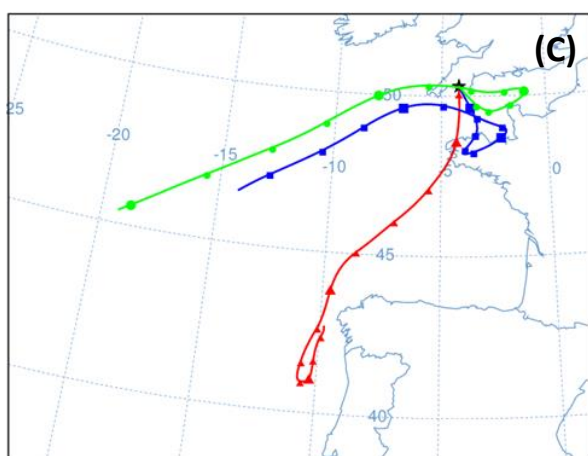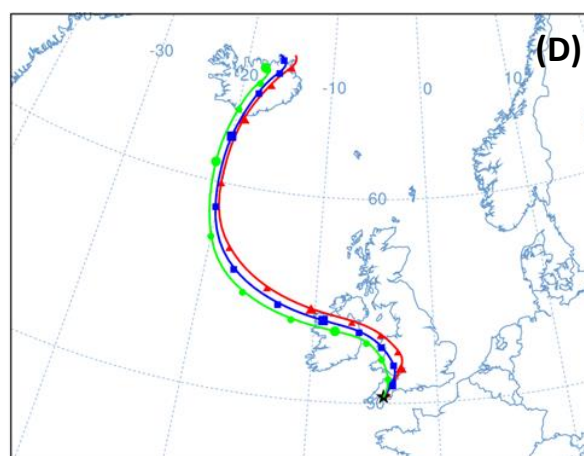and marine emissions (Channel Mixed).

Figure 2: *Example back trajectories for the four sectors defined for this study. Multiple trajectories*

were run per sample (different colour lines). Symbols represent 6 hour intervals along the trajectory.

3. RESULTS

3.1 Penlee Point Atmospheric Observatory Aerosols

214   Air mass NO_3^- concentrations varied from 2–366 nmol N m^{-3}, with the minimum and maximum

215   occurred on 26th February and 9th April, respectively (Figure 3; Figure 4). The highest aerosol NO_3^-

216   concentrations were observed in air masses from continental Europe/UK Mainland, and these were

217   associated with an easterly local wind direction (Figure 4). NO_3^- concentrations associated with this

218   source region also had the greatest concentration range (128 – 366 nmol N m^{-3}). In contrast, low

219   aerosol NO_3^- concentrations were observed in North Atlantic clean aerosols (2–27 nmol N m^{-3}) except

220   on the 16th June (43 nmol N m^{-3}). Low wind speeds prevailed during sample collection on the 16th June,

221   and the back trajectory suggests that the air mass circulated over the Celtic Sea and English Channel.

222   Hence it is likely this aerosol sample had entrained emissions from the intense shipping activity in
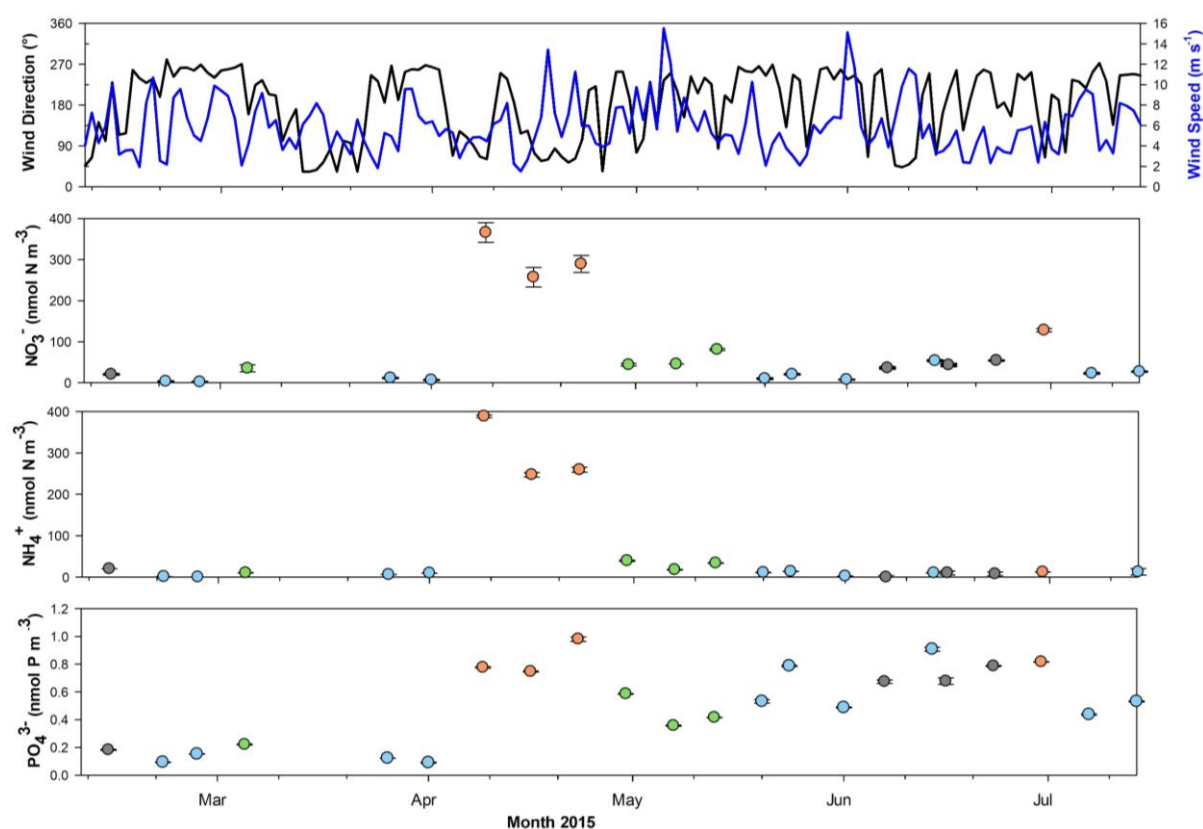
223   these waters.

224

225   **Figure 3:** *Timeseries of aerosol inorganic N (NO_3^- and NH_4^+, nmol N m^{-3}) and PO_4^{3-} (nmol P m^{-3})*

226   *concentrations, wind speed (m s^{-1}) and local wind direction (degrees) between 9th February and 14th*

227   *July 2015. Points are coloured by source region classification: North Atlantic Clean (blue), Continental*

(orange), Channel Mixed (green) and North Atlantic Mixed (grey). Major tick marks represent the 1st

229 *of the month and minor tick marks represent 10th and 20th days.*

230 Aerosol NH_4^+ concentrations ranged from 0.21 – 389 nmol N m^{-3} and tended to co-vary with NO_3^-

231 concentrations (Figure 3). Continental aerosols had the highest NH_4^+concentrations. One exception

232 was on 30th June 2015, when NH_4^+ concentrations were 12.2 nmol N m^{-3}, which is more comparable

233 with background North Atlantic samples than with other Continental samples. The NO_3^- concentration

234 in the same sample was approximately 50% of the other three Continental samples. Back trajectory

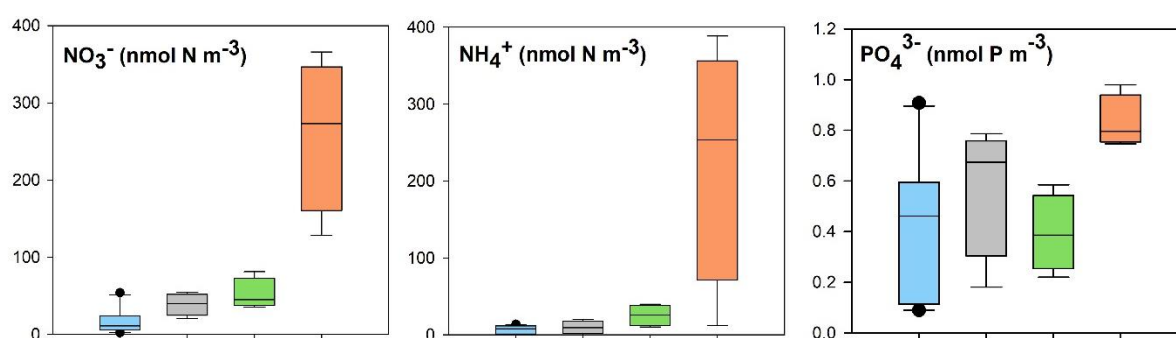235 analysis shows that the air had circulated in the English Channel for 72 hours prior to sampling.

236

237 **Figure 4**: *Box and whisker plots of aerosol NO_3^-, NH_4^+ and PO_4^{3-} concentrations, coloured by source*

238 *region classification: North Atlantic clean (blue, 10 samples), Continental (orange, 4 samples), Channel*

239 *Mixed (green, 4 samples) and North Atlantic Mixed (grey, 4 samples).*

240

241 Aerosol phosphate (PO_4^{3-}) concentration ranged from 0.1 – 1.0 nmol P m^{-3}. The lowest concentrations

242 were recorded on 21st February and 1st April 2015, and the highest occurred on 23rd April (Figure 4).

243 PO_4^{3-} was considerably less abundant than aerosol nitrogen, and there was no clear link between the

244 PO_4^{3-} concentrations and air mass classification or variations in inorganic nitrogen concentration.

245 Mineral and soil dusts are the major source of soluble P for aerosol. These are typically larger particles

246 with short atmospheric residence times. Thus, atmospheric P concentrations are likely to be

247 dependent on localised continental sources rather than long range transport (Myriokefalitakis *et al.*,

248 2016). Average (mean and median) aerosol PO_4^{3-} concentrations in air masses from the European

249 Continent/UK were elevated (Figure 4) compared to other source regions, especially North Atlantic

250 Clean and Channel Mixed. Concentrations from the North Atlantic Mixed region were also slightly

251 elevated, suggesting terrestrial influence as the trajectories passed over South West England and
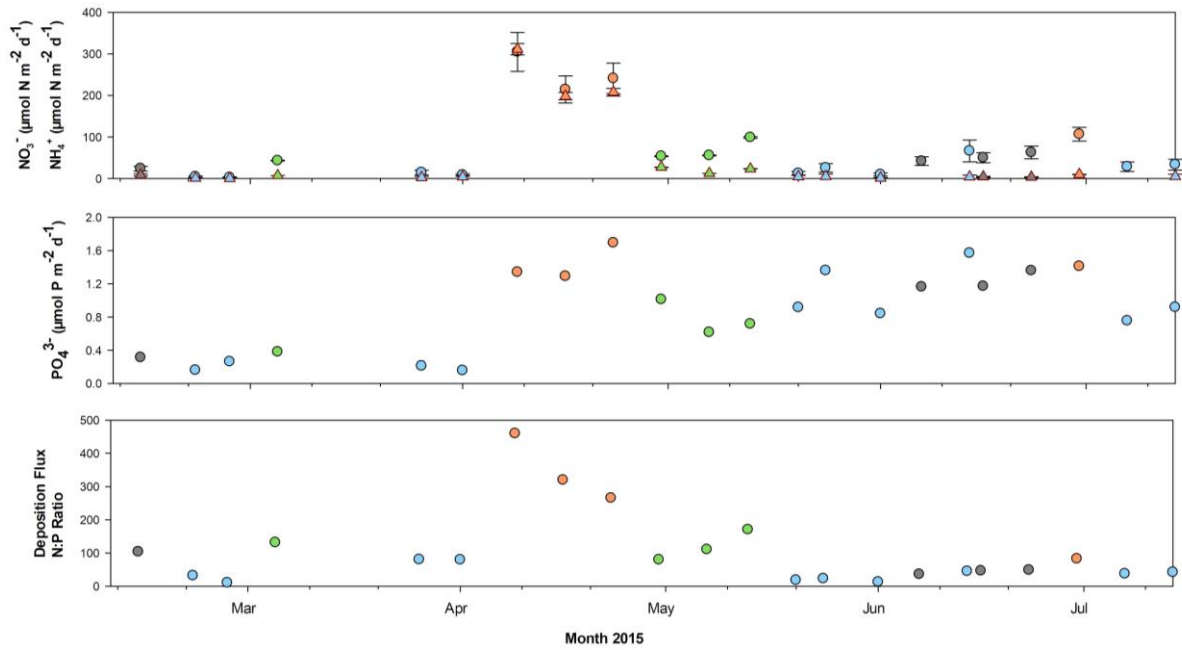
252 South East Ireland.

253

254 **Figure 5:** *Dry deposition fluxes for NO_3^-, NH_4^+ and PO_4^{3-} (μmol N/P m^{-2} d^{-1}) and the N:P ratio of the*

255 *aerosol depositing on the sea surface. Circles and triangles in the top panel represent nitrogen fluxes*

256 *resulting from NO_3^- and NH_4^+ respectively. Points are coloured by back trajectory source regions: North*

257 *Atlantic Clean (blue), Continental (orange), Channel Mixed (green) and North Atlantic Mixed (grey).*

258 *Error bars on NO_3^- and NH_4^+ show the maximum/minimum deposition using the coarse/fine size*

259 *distribution ranges in Table 1. Major tick marks represent the 1st of the month and minor tick marks*

260 *represent 10th and 20th days.*

261 Average NO_3^- and NH_4^+ deposition flux were 68 ($\pm$ 12) and 38 ($\pm$ 3) μmol N m^{-2} d^{-1} respectively.

262 Deposition fluxes ranged from 3 ($\pm$ 1) to 300 ($\pm$ 47) μmol N m^{-2} d^{-1} for NO_3^- and 0.01 ($\pm$ 0.03) to 310

263 ($\pm$14) μmol N m^{-2} d^{-1} for NH_4^+. The N:P ratio of the aerosol deposition flux (Figure 5) demonstrates that

264   N deposition far exceeds P deposition, with most samples exceeding 50:1 N:P ratio. Only 1 sample

265   period had an N:P ratio in the deposited aerosol that fell below the Redfield ratio in seawater (16:1) .

266   **3.2 Trends in marine mixed layer nutrients in the Western English Channel**

267   Vertical nutrient profiles from the Western Channel Observatory L4 marine time series site were

268   integrated down to the base of the spring/summer mixed layer. A pycnocline formed during spring

269   from May onwards, and the average depth was 16 m (± 11 m). A mixed layer depth was defined for

270   each profile using a ± 0.03 kg m^3 density difference starting at 3 m. Nutrient profiles were integrated

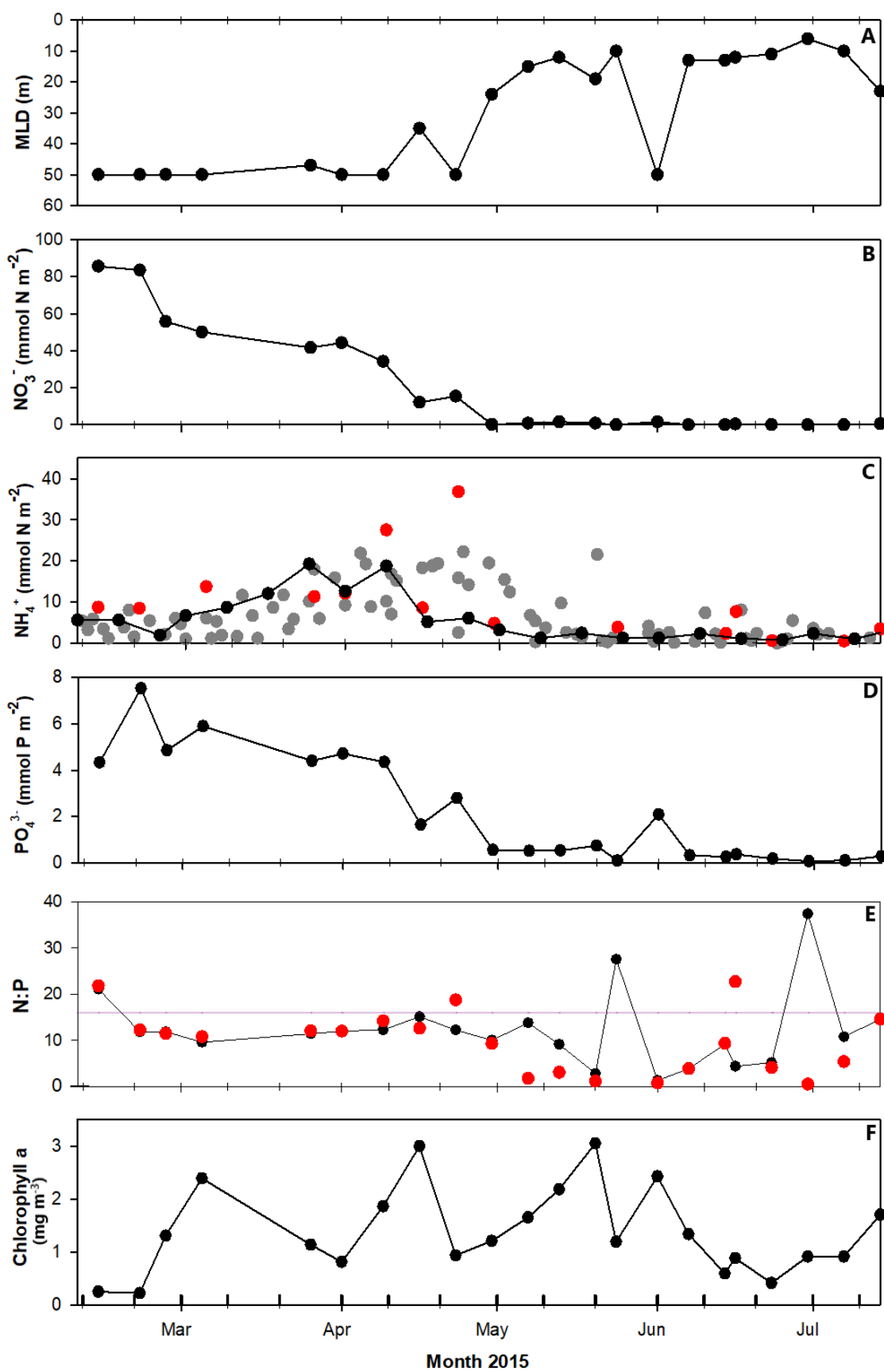271   down to the seabed (54 m) prior to stratification (Figure 6).

273 **Figure 6:** *WCO L4 timeseries for spring bloom period in 2015. (A) Mixed layer depth used for nutrient*

274 *integration, derived as +/- 0.03 kg m^{-3} from density profiles calculated from CTD temperature & salinity*

275 *profiles (1 atm) starting at 3m. (B, C, D) Integrated mixed layer nutrient concentrations (NO$_3^-$, NH$_4^+$,*

276 *PO$_4^{3-}$), (E) mixed layer N:P ratio and (F) Chlorophyll a (mg m^{-3}) concentration at the surface. Grey dots*

277 *on NH$_4^+$ plot are data from 2016-2019, red dots are for data from 2015 and the black dots/black line*

278 *shows the median trend of all these NH$_4^+$ data. Major tick marks represent the 1st of the month and*

279 *minor tick marks represent 10th and 20th days.*

280 The water column was fully mixed at the WCO between 9th February and 7th April 2015. Stable

281 stratifications occurred April 30th at which point the mean mixed layer depth (MLD) was 17 m (± 11

282 m). Stratification was broken down once during the bloom season on June 1st. Mixed layer nutrients

283 reduced significantly during the spring/summer months, reflecting the typical seasonal pattern of

284 phytoplankton growth and nutrient utilisation in these waters (Statham *et al.,* 2012). Mixed layer NO$_3^-$

285 ranged from 0.01–85.6 mmol N m^{-2}, with minima and maxima measured on 7th June and 9th February,

286 respectively (Figure 6). NO$_3^-$ decreased to a low level (< 5 nmol N m^{-2}) on 27th April 2015 and remained

287 low for the remainder of the campaign.

288 Surface layer NH$_4^+$ ranged from 0.5 - 36.8 mmol N m^{-2} and did not follow exactly the same trend as

289 NO$_3^-$ (Figure 6). Water column measurements of NH$_4^+$ during the 2015 campaign were inconsistently

290 reported after the water column stratifies (Figure 6). To mitigate this uncertainty, a median seasonal

291 trend for NH$_4^+$ concentrations was derived from all available WCO data from 2015 – 2019 (Figure 6).

292 There are three distinct stages to the seasonal NH$_4^+$ concentration changes: (i) concentrations are low

293 until mid-March because, unlike NO$_3^-$ and PO$_4^-$, winter stocks are low; (ii) NH$_4^+$ concentrations increase

294 almost three fold at the onset of the spring bloom and before stratification, with some inter-annual

295 variation, indicating a biological turnover source of NH$_4^+$, e.g. NH$_4^+$ production due to grazing by

296 zooplankton communities (Alcaraz, Saiz & Estrada, 1994); (iii) concentration decline to winter levels

297 after stratification, with occasional spikes, possibly due to secondary blooms or another point source

298 (e.g. river Tamar inputs).

299 Surface layer PO_4^{3-} ranged from 0.06 to 7.5 mmol P m^{-2}, with the minimum and maximum measured

300 on 30th June and February 9th 2015, respectively. The decline in PO_4^{3-} levels reflects the seasonal

301 nutrient depletion also observed in the dissolved inorganic nitrogen (DIN, = NO_3^-+ NH_4^+) levels (Figure

302 6). The majority of observed N:P ratios at the WCO L4 site were below the expected Redfield ratio (i.e.

303 < 16:1), meaning that PO_4^{3-} was predominately in excess (Figure 6). Excess PO_4^{3-} indicates that, with

304 sufficient light, addition of N to the system could stimulate greater biological productivity. Only when

305 there are elevated NH_4^+ concentrations in the water column does the N:P ratio rise above 16, which

306 could have led to P limitation within the phytoplankton community. P-limitation (or stress) at the WCO

307 has been measured previously following an influx of N-rich fresh water from the River Tamar, through

308 an increase in alkaline phosphatase activity (Rees *et al.,* 2009).

4. DISCUSSION

310 The N dry deposition fluxes presented in this study are of a similar magnitude to measurements

311 elsewhere in western Europe during the past 20 years. Nitrogen (NO_3^- + NH_4^+) dry deposition flux at

312 PPAO ranged from 2.7 (± 1.1) to 620 (± 60) μmol N m^{-2} d^{-1}, which is similar to the range reported from

313 a coastal atmospheric station in De Haan, Belgium (7.86 – 405 μmol N m^{-2} d^{-1}; (Bencs *et al.*, 2009)).

314 The large N dry deposition event from 9th-23rd April 2015 was much higher than the fluxes observed

315 during the 1996/1997 sampling campaign at Mace Head, Ireland (9.3–203 μmol N m^{-2} d^{-1} (Spokes *et*

316 *al.*, 2000)). PPAO is closer than Mace Head to continental Europe, which may explain this difference.

317 Yeatman *et al*, (2001) collected aerosols from continental air masses at Weybourne (on the coast of

318 the North Sea, South East UK). The authors observed dry deposition fluxes between 166 and 1545

319 μmol N m^{-2} d^{-1}. Weybourne and the southern North Sea are very close (< 400 km) to the industrial

320 heartland of mainland Europe and thus more exposed than the PPAO/WCO to large N deposition

321 events. Other factors will have influenced the observations outlined above, including: (i) time that air

322   masses spend over industrial and agricultural regions; (ii) changing emission source strengths; (iii)

323   different relative proportions of wet versus dry deposition; and (iv) different atmospheric chemical

324   and physical processing.

325   Minimum NO_3^- and NH_4^+ concentrations were observed in North Atlantic Clean air masses. Maximum

326   NO_3^- and NH_4^+ concentrations were observed when air came from Continental Europe (Figure 4).

327   Interestingly, though NO_3^- and NH_4^+ emission sources are different, we observed that aerosol

328   concentrations in Continental Europe samples co-varied and had a relatively constant 1:1 ratio (See

329   Supplementary material). The aerosol concentration ratio may be determined by a similar average

330   ratio in the emissions from the European continent. Indeed, estimated N emissions from continental

331   European countries reported that annual average oxidised and reduced N emissions were also

332   approximately 1:1 (Leip *et al.,* 2011). Several samples were noted to have back trajectories that

333   traverse regions of high shipping density, which will contribute additional NO_3^- but not NH_4^+(Hertel *et*

334   *al.*, 2012). In contrast with inorganic N fluxes, PO_4^{3-} dry deposition flux varied far less (one order of

335   magnitude), most likely due to a more consistent local source in the form of mineral dusts and soils,

336   rather than an integrated concentration over greater transport distances. Marine sources are not as

337   significant: Baker *et al.*, (2010) reported only 0.98– 4.89 nmol P m^{-2} d^{-1} dry phosphate fluxes in the

338   middle of the North Atlantic Ocean (~3 orders of magnitude lower than this study). The significant

339   difference is likely due to the proximity of PPAO to crustal source material and the association of PO_4^{3-}

340   with coarse mode aerosols that have a much shorter atmospheric residence time (Duce *et al.*, 1991).

341   PO_4 concentrations are low when polluted air masses came from Continental Europe, possibly because

342   the low residence time of larger dust aerosols reduces the significance of non-arid source regions far

343   from the sampling site. Furthermore, PO_4^{3-} airmass concentrations are typically low and it is

344   challenging to accurately distinguish between the relative contribution of natural and anthropogenic

345   sources to the low levels of aerosol PO_4^{3-} measured in this study.

346   **Impact of atmospheric aerosol deposition on surface mixed layer nutrients**

347   Oceanic data from the WCO L4 marine time-series station and atmospheric data from the PPAO were

348   used to assess the potential impact of aerosol nutrients on the local seawater (Figure. 7). As an

349   indicator, a simple 1-D approach to compare the atmospheric aerosol N flux in one day ($DIN_{Aerosol}$) to

350   the standing stock of DIN integrated to the base of the MLD/seabed (DIN_{ML}) as a percentage (*%DIN*):

351 $$\%DIN = 100 \times DIN_{Aerosol}/DIN_{ML} \qquad (2)$$

352   This approach was initially applied to dry aerosol PO_4^{3-} deposition but the contributions were

353   consistently below 0.1 %. Therefore, all further discussion of the response of the WCO L4 site to

354   aerosol nutrient deposition and the potential biogeochemical consequences will focus on N

355   deposition.

356   The water column was mixed down to the seabed prior to 13th April 2015, and DIN_{ML} levels were high

357   (>10 mmol N m^{-2}) such that aerosol deposition had very little impact on seawater DIN (*%DIN* < 1 %,

358   Figure 7). The onset of stratification around 1st May 2015 led to strong biological uptake and reduced

359   DIN_{ML} levels to below 10 mmol N m^{-2}. The $DIN_{Aerosol}$ in early May was classified as Channel Mixed and

360   this aerosol contributed up to 8% of DIN_{ML}. DIN_{ML} was almost completely depleted (< 10 mmol N m^{-2})

361   during June 2015 and after this time, deposition events resulted in %DIN exceeding 20% (Figure 7).
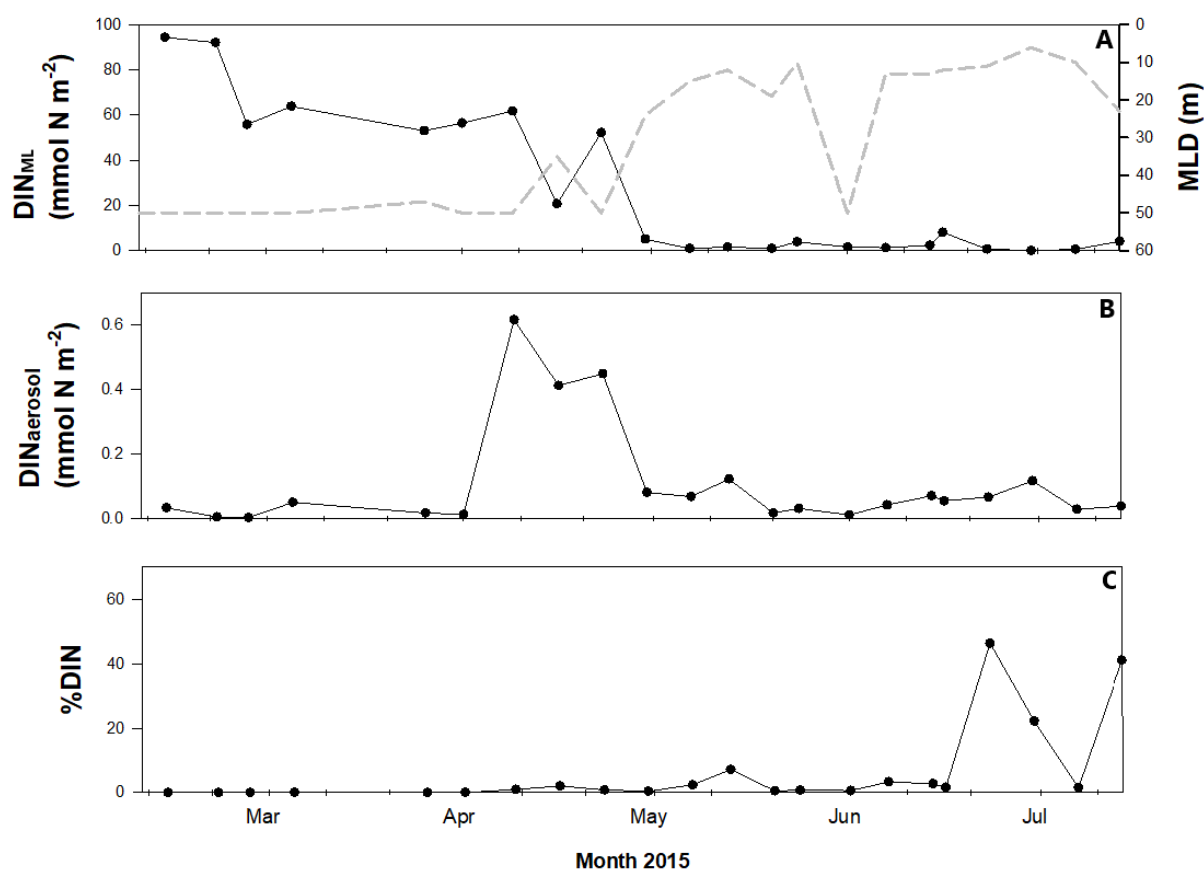
362

Figure 7: *Timeseries of: (A)Mixed layer dissolved inorganic nitrogen (DIN_{ML}), grey line is MLD used for integration; (B) total aerosol dry nitrogen deposition flux ($DIN_{Aerosol}$); and (C) contribution of dry deposition to water column inorganic N (%DIN, see text for how calculated). Major tick marks represent the 1st of the month and minor tick marks represent 10th and 20th days.*

367   The deposition event on June 30th 2015 had the biggest potential impact and contributed almost 23 %

368   of DIN_{ML} at the WCO L4 station (Figure 7). Remarkably, %DIN was not significant during the very high

369   $DIN_{Aerosol}$ deposition events (Continental air masses) in April 2015 because the water was not yet

370   stratified and nutrient stocks were not depleted (Figure 7). Thus, sporadic atmospheric aerosol N

371   deposition can be significant source of nitrogen to shelf waters when DIN_{ML} is depleted during periods

372   of stratification and intense biological activity. Atmospheric circulation patterns are not tied to the

373   onset of stratification, however previous studies from PPAO have shown that winter dominance of

374   SW (marine) air masses is reduced in spring/summer allowing for more Continental air masses to occur

20

375 (Yang *et al.,* 2019; Yang *et al.*, 2016a; Yang *et al.*, 2016b). Had the high $DIN_{Aerosol}$ inputs occurred in May

376 rather than in April, the *%DIN* would have been 14–37 %. Therefore, continental air masses have the

377 potential to significantly influence the late spring and summer phytoplankton bloom at the WCO.

378 Another relative comparison can be made between aerosol deposition and vertical water column

379 fluxes across the seasonal thermocline to the mixed layer. Summertime diffusive fluxes of NO_3^- across

380 the stratified thermocline in the nearby Celtic Sea are 1.8 – 2 mmol NO_3^- m^{-2} d^{-1} (Birchill *et al*., 2017;

381 Sharples *et al*., 2009). Hence the maximum dry deposition event observed at PPAO was equivalent to

382 around a third of the typical daily diffusive flux across the thermocline.

383 **Carbon fixation due to aerosol deposition into coastal waters**

384 The assimilation of one mole of reactive nitrogen leads to 6.625 moles of carbon assimilation

385 according to Redfield stoichiometry (106C : 16N : 1P; (Geider and La Roche, 2002; Redfield, 1958)).

386 To calculate carbon fixation related to aerosol N deposition, we assume that all $DIN_{Aerosol}$ was

387 bioavailable and that the other requirements for biological growth (other macro- and micro-nutrients,

388 light, temperature) were met. The $DIN_{Aerosol}$ contribution of 0.02 – 0.62 mmol N m^{-2} d^{-1} during this

389 study was potentially able to support 0.01 – 4.36 mmol C m^{-2} d^{-1} of carbon uptake (Figure 8A).

390 Previous studies have compared the potential carbon fixation due to $DIN_{Aerosol}$ to the seasonal average

391 carbon fixation in the North Atlantic Ocean (Bencs et al., 2009, Spokes and Jickells, 2005). These

392 studies observed that dry N deposition derived from continental European air masses could account

393 for up to 15 % of the daily C fixation in the N E Atlantic Ocean (Bencs et al., 2009, Spokes and Jickells,

394 2005). Barnes *et al.,* (2015) report seasonal C-fixation rates and estimates for the WCO L4 station

395 between 2003 and 2010. The average C- fixation rate during the season phytoplankton bloom at the

396 WCO is 43.3 mmol C m^{-2} d^{-1} (Barnes *et al.,* 2015). We estimate C-fixation at the WCO L4 site (PP$_o$) using

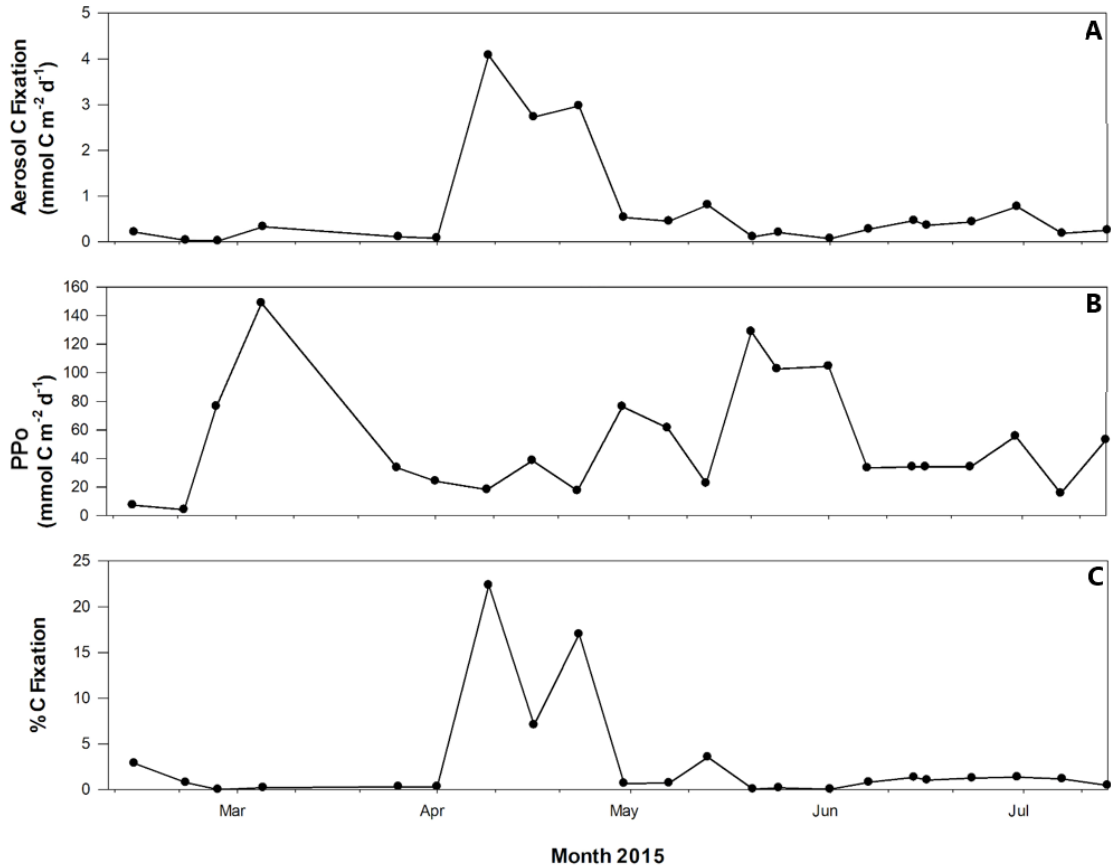397 in situ chlorophyll observations (Barnes *et al*., 2014) (Figure 8B):

398   α_{ph} = 0.0134 x Chl a x 0.0075   (3)

399                                    $PP_o = 0.0109 \times (\alpha_{ph} \times E_{par}) - 0.00018$ (4)

400   Where α_{ph} is absorption coefficient of phytoplankton, and E_{par} is photosynthetically active radiation.

401

402   **Figure 8:** *Timeseries of: (A) Carbon fixation due to DIN$_{Aerosol}$ input (Cfix$_{Aerosol}$), assuming uptake follows*

403   *the phytoplankton Redfield ratio; (B) Carbon fixation (PP$_o$) at the Western Channel Observatory L4*

404   *station estimated from in situ observations (see Eqn. 3); and (C) Proportion of PP$_o$ at L4 that could be*

405   *supported by atmospheric N deposition, assuming all DIN$_{Aerosol}$ is bioavaliable (%Cfix = 100 x Cfix$_{Aerosol}$ /*

406   *PP$_o$). Major tick marks represent the 1st of the month and minor tick marks represent 10th and 20th*

407   *days.*

408   We compared C-fixation (*PP$_o$*) at the WCO with the C-fixation that could potentially be supported by

409   aerosol N deposition (*Cfix$_{Aerosol}$*) using *%Cfix = 100 x Cfix$_{Aerosol}$/PP$_o$* (Figure 8C). The typical *%Cfix* was

410   ~1%. The *%Cfix* resulting from continental aerosol deposition during April was 15.5% on average, with

411 dry N deposition on April 9th potentially able to support a substantial amount of the mixed layer carbon

412 fixation (*%Cfix = 22.4%*).

413 Overall, these recent data highlight the continuation of high sporadic atmospheric nitrogen fluxes

414 originating from air circulation over highly populated land masses and the impact they can have on

415 surface ocean biogeochemistry. Spokes and Jickells, (2005) also reported significant wet and dry

416 nitrogen deposition (0.8 mmol m^{-2} d^{-1}) at Mace Head, Ireland, when air had been transported over the

417 European continent. Bencs *et al.,* (2009) reported a similar magnitude deposition event at De Haan,

418 Belgium. Both studies calculate that episodic deposition events containing polluted European aerosol

419 could support ~15 % of total surface water carbon fixation (Bencs et al., 2009, Spokes and Jickells,

420 2005). The magnitude of N deposition is a function of both location (proximity to aerosol N sources)

421 and prevailing wind direction. Neither of the events observed in Ireland or Belgium deposited as much

422 N as the PPAO event on April 9th 2015.

423 **Impact of N Deposition on Atlantic Shelf Waters**

424 In the previous sections the impact of dry N deposition to the coastal shelf waters near PPAO have

425 been evaluated and revealed two separate conclusions. While the carbon fixation estimates the

426 deposition events in April (corresponding to the highest atmospheric aerosol N concentrations) to

427 have the greatest impact, this was not the case when those deposition events were compared to the

428 standing nutrient stocks. From that investigation we conclude that N deposition has the most impact

429 once the nutrient stocks are depleted during the summer (June onwards) bloom season. Considered

430 together these calculations show that the impact of dry N deposition can have significance, but only

431 when certain conditions are met. However this also highlights the complexity of the cycling of

432 nutrients from the atmospheric into marine surface waters, and there are certainly other factors to

433 investigate in future work at this study site. For instance, the calculation we used to estimate the

434 contribution of $DIN_{Aerosol}$ to DIN_{ML} (Eqn. 2) assumes that DIN_{ML} is at steady state and does not consider

435 the potential importance of other N input and output terms due to uptake and removal processes.

436   Riverine input, atmospheric wet deposition, and diffusive fluxes of nitrogen across the thermocline

437   may all influence DIN cycling in WCO waters.

438   Rainfall will play an important role for coastal and shelf N deposition during the seasons. For example,

439   heavy rainfall over the River Tamar catchment has been shown to increase the freshwater flux of DIN

440   into the English Channel, influencing the WCO L4 site. DIN concentrations at L4 after freshwater influx

441   events in 2007 increased by 1.78 ± 0.20 µmol L^{-1}, coinciding with lowered salinity and increased P

442   stress (Rees *et al.,* 2009).

443   Preliminary NO_3^- data in rainwater from PPAO show concentrations in the range of 5.6 - 49 µmol L^{-1}.

444   Rainfall efficiently scavenges atmospheric aerosol such that wet N deposition is typically greater than

445   dry N deposition and is likely to add a further significant seasonal flux to the shelf nitrogen budget.

446   The studies in Ireland and Belgium measured twofold higher flux of wet deposition than dry deposition

447   (Bencs *et al*., 2009, Spokes and Jickells, 2005). Thus, the total atmospheric N deposition in the WCO

448   during our study would have been of higher magnitude if rainfall were considered, particularly as there

449   were 9 major rain events at the PPAO during April 2015. Furthermore, organic N aerosol was not

450   measured in this study, but reports from elsewhere suggest that it may represent 15 – 65 % of the

451   total atmospheric N budget (e.g., Jickells *et al.*, 2013), so the effect of organic N deposition on marine

452   biogeochemistry is likely to be even larger. Thus, the combined impact of dry plus wet N deposition

453   and additional fluxes of organic nitrogen on shelf water biogeochemistry, clearly warrant further

454   investigation.

455   **5. Conclusions**

456   This study investigated atmospheric aerosol N and P, their sources and the potential impact on surface

457   water biogeochemistry at the WCO between February and July 2015. The highest concentrations of N

458   in aerosol were linked to pollution sources in continental Europe. These aerosol samples contained

459   significantly more N than samples from other source regions, and likely contribute substantial pulses

460   of new N into surface waters at the WCO. These shelf waters were N-limited throughout the spring

461   bloom season, and severe N-depletion generally occurred after the onset of water column

462   stratification in spring. Aerosol N deposition always exceeded aerosol P deposition (N:P ratio > 250 in

463   polluted continental European air mass samples) and N:P was also greater than the typical seawater

464   ratio (i.e., Redfield >16:1). Calculations demonstrate that aerosol-derived had the greatest impact on

465   biological productivity in shelf waters once the water column became stratified and during sustained

466   winds from mainland Europe, more than 20 % of water column carbon fixation can be supported by

467   aerosol N deposition.

468

480

481 # References

482   Alcaraz, M., Saiz, E. & Estrada, M. (1994) 'Excretion of ammonia by zooplankton and its potential

483   contribution to nitrogen requirements for primary production in the Catalan Sea (NW

484   Mediterranean)'. *Marine Biology*, 119 (1), pp. 69-76.

485

486 Baker, A. R. and Jickells, T. D. (2017) 'Atmospheric deposition of soluble trace elements along the

487 Atlantic Meridional Transect (AMT)', *Progress in Oceanography,* 158, pp. 41-51.

488

489 Baker, A. R., Lesworth, T., Adams, C., Jickells, T. D. & Ganzeveld, L. (2010) 'Estimation of atmospheric

490 nutrient inputs to the Atlantic Ocean from 50°N to 50°S based on large-scale field sampling: Fixed

491 nitrogen and dry deposition of phosphorus'. *Global Biogeochemical Cycles*, 24 (3),

492

493 Baker, A. R., Weston, K., Kelly, S. D., Voss, M., Streu, P. & Cape, J. N. (2007) 'Dry and wet deposition of

494 nutrients from the tropical Atlantic atmosphere: Links to primary productivity and nitrogen fixation'.

495 *Deep Sea Research Part I: Oceanographic Research Papers*, 54 (10), pp. 1704-1720.

496

497 Baker, A. R., Jickells, T. D., Biswas, K. F., Weston, K. and French, M. (2006) 'Nutrients in atmospheric

498 aerosol particles along the Atlantic Meridional Transect', *Deep Sea Research Part II: Topical Studies in*

499 *Oceanography,* 53(14–16), pp. 1706-1719.

500

501 Barnes, M. K., Tilstone, G. H., Suggett, D. J., Widdicombe, C. E., Bruun, J., Martinez-Vicente, V. & Smyth,

502 T. J. (2015) 'Temporal variability in total, micro- and nano-phytoplankton primary production at a

503 coastal site in the Western English Channel'. *Progress in Oceanography*, 137 pp. 470-483.

504

505 Barnes, M. K., Tilstone, G. H., Smyth, T. J., Suggett, D. J., Astoreca, R., Lancelot, C. and Kromkamp, J. C.

506 (2014) 'Absorption-based algorithm of primary production for total and size-fractionated

507 phytoplankton in coastal waters', *Marine Ecology Progress Series,* 504, pp. 73-89.

508

509 Bencs, L., Krata, A., Horemans, B., Buczyńska, A. J., Dirtu, A. C., Godoi, A. F. L., Godoi, R. H. M.,

510 Potgieter-Vermaak, S. & Van Grieken, R. (2009) 'Atmospheric nitrogen fluxes at the Belgian coast:

511 2004–2006'. *Atmospheric Environment*, 43 (24), pp. 3786-3798.

512

513 Birchill, A. J., Clinton-Bailey, G., Hanz, R., Mawji, E., Cariou, T., White, C., Ussher, S. J., Worsfold, P. J.,

514 J, Achterberg, E., P and Mowlem, M. (2019) 'Realistic measurement uncertainties for marine

515 macronutrient measurements conducted using gas segmented flow and Lab-on-Chip

516 techniques', *Talanta,* 200, pp. 228-235.

517

518 Birchill, A. J., Milne, A., Woodward, E. M. S., Harris, C., Annett, A., Rusiecka, D., Achterberg, E. P.,

519 Gledhill, M., Ussher, S. J., Worsfold, P. J., Geibert, W. and Lohan, M. C. (2017) 'Seasonal iron depletion

520 in temperate shelf seas', *Geophysical Research Letters,* 44(17), pp. 8987-8996.

521

522 Björkman, K. M. & Karl, D. M. (2003) 'Bioavailability of dissolved organic phosphorus in the euphotic

523 zone at Station ALOHA, North Pacific Subtropical Gyre'. *Limnology and Oceanography*, 48 (3), pp.

524 1049-1057.

525

526 Chester, R. & Jickells, T. (2012) 'The Transport of Material to the Oceans: The Atmospheric Pathway',

527 *Marine Geochemistry.* John Wiley & Sons, Ltd, pp. 52-82.

528

529 Cornell, S. E. & Jickells, T. D. (1999) 'Water-soluble organic nitrogen in atmospheric aerosol: a

530 comparison of UV and persulfate oxidation methods'. *Atmospheric Environment*, 33 (5), pp. 833-840.

531

532 Duce, R. A., LaRoche, J., Altieri, K., Arrigo, K. R., Baker, A. R., Capone, D. G., Cornell, S., Dentener, F.,

533 Galloway, J., Ganeshram, R. S., Geider, R. J., Jickells, T., Kuypers, M. M., Langlois, R., Liss, P. S., Liu, S.

534 M., Middelburg, J. J., Moore, C. M., Nickovic, S., Oschlies, A., Pedersen, T., Prospero, J., Schlitzer, R.,

535 Seitzinger, S., Sorensen, L. L., Uematsu, M., Ulloa, O., Voss, M., Ward, B. & Zamora, L. (2008) 'Impacts

536 of Atmospheric Anthropogenic Nitrogen on the Open Ocean'. *Science*, 320 (5878), pp. 893-897.

537

538 Duce, R. A., Liss, P. S., Merrill, J. T., Atlas, E. L., Buat-Menard, P., Hicks, B. B., Miller, J. M., Prospero, J.

539 M., Arimoto, R., Church, T. M., Ellis, W., Galloway, J. N., Hansen, L., Jickells, T. D., Knap, A. H., Reinhardt,

540 K. H., Schneider, B., Soudine, A., Tokos, J. J., Tsunogai, S., Wollast, R. & Zhou, M. (1991) 'The

541 atmospheric input of trace species to the world ocean'. *Global Biogeochemical Cycles*, 5 (3), pp. 193-

542 259.

543

544 Elser, J. J., Bracken, M. E. S., Cleland, E. E., Gruner, D. S., Harpole, W. S., Hillebrand, H., Ngai, J. T.,

545 Seabloom, E. W., Shurin, J. B. & Smith, J. E. (2007) 'Global analysis of nitrogen and phosphorus

546 limitation of primary producers in freshwater, marine and terrestrial ecosystems'. *Ecology Letters*, 10

547 (12), pp. 1135-1142.

548 Galloway, J. N., Aber, J. D., Erisman, J. W., Seitzinger, S. P., Howarth, R. W., Cowling, E. B. & Cosby, B.

549 J. (2003) 'The Nitrogen Cascade'. *Bioscience*, 53 (4), pp. 341-356.

550

551 Gardolinski, P. C. F. C., Hanrahan, G., Achterberg, E. P., Gledhill, M., Tappin, A. D., House, W. A. &

552 Worsfold, P. J. (2001) 'Comparison of sample storage protocols for the determination of nutrients in

553 natural waters'. *Water Research*, 35 (15), pp. 3670-3678.

554

555 Geider, R. & La Roche, J. (2002) 'Redfield revisited: variability of C:N:P in marine microalgae and its

556 biochemical basis'. *European Journal of Phycology*, 37 (1), pp. 1-17.

557

558 Hansen, H. P. & Koroleff, F. (2007) 'Determination of nutrients', *Methods of Seawater Analysis.* Wiley-

559 VCH Verlag GmbH, pp. 159-228.

560

561 Hertel, O., Skjøth, C. A., Reis, S., Bleeker, A., Harrison, R. M., Cape, J. N., Fowler, D., Skiba, U., Simpson,

562 D., Jickells, T., Kulmala, M., Gyldenkærne, S., Sørensen, L. L., Erisman, J. W. & Sutton, M. A. (2012)

563 'Governing processes for reactive nitrogen compounds in the European atmosphere'. *Biogeosciences*,

564 9 (12), pp. 4921-4954.

565

566 Holmes, R. M., Aminot, A., Kérouel, R., Hooker, B. A. & Peterson, B. J. (1999) 'A simple and precise

567 method for measuring ammonium in marine and freshwater ecosystems'. *Canadian Journal of*

568 *Fisheries and Aquatic Sciences*, 56 (10), pp. 1801-1808.

569

570 Jickells, T. D., Buitenhuis, E., Altieri, K., Baker, A. R., Capone, D., Duce, R. A., Dentener, F., Fennel, K.,

571 Kanakidou, M., LaRoche, J., Lee, K., Liss, P., Middelburg, J. J., Moore, J. K., Okin, G., Oschlies, A., Sarin,

572 M., Seitzinger, S., Sharples, J., Singh, A., Suntharalingam, P., Uematsu, M. & Zamora, L. M. (2017) 'A

573 reevaluation of the magnitude and impacts of anthropogenic atmospheric nitrogen inputs on the

574 ocean'. *Global Biogeochemical Cycles*, 31 (2), pp. 289-305.

575

576 Kim, T.-W., Lee, K., Duce, R. & Liss, P. (2014) 'Impact of atmospheric nitrogen deposition on

577 phytoplankton productivity in the South China Sea'. *Geophysical Research Letters*, 41 (9), pp. 3156-

578 3162.

579

580 Kocak, M. (2015) 'Solubility of Atmospheric Nutrients over the Eastern Mediterranean: Comparison

581 between Pure-Water and Sea-Water, Implications Regarding Marine Production', *Turkish Journal of*

582 *Fisheries and Aquatic Sciences,* 15, pp. 59-71.

583

584 Krishnamurthy, A., Moore, J. K., Mahowald, N., Luo, C., Doney, S. C., Lindsay, K. & Zender, C. S. (2009)

585 'Impacts of increasing anthropogenic soluble iron and nitrogen deposition on ocean biogeochemistry'.

586 *Global Biogeochemical Cycles*, 23 (3), pp. n/a-n/a.

587

588   Leip, A., Achermann, B., Billen, G., Bleeker, A., Bouwman, A. F., De Vries, W., Dragosits, U., Döring, U.,

589   Fernall, D., Geupel, M., Herolstab, J., Johnes, P., Le Gall, A. C., Monni, S., Nevečeřal, R., Orlandini, L.,

590   Prud'homme, M., Reuter, H. I., Simpson, D., Seufert, G., Spranger, T., Sutton, M. A., Van Aardenne, J.,

591   Voß, M. & Winiwarter, W. (2011) 'Integrating nitrogen fluxes at the European scale', in Sutton, M.A.,

592   Howard, C.M., Erisman, J.W., Billen, G., Bleeker, A., Grennfelt, P., Van Grinsven, H. and Bruna, G. (eds.)

593   *The European Nitrogen Assessment: Sources, Effects and Policy Perspectives.* Cambridge: Cambridge

594   University Press.

595

596   Lentz, S., Shearman, K., Anderson, S., Plueddemann, A. and Edson, J., (2003) 'Evolution of

597   stratification over the New England shelf during the Coastal Mixing and Optics study, August 1996–

598   June 1997.' *Journal of Geophysical Research*, 108 (C1), pp. 1-14

599

600   Lesworth, T., Baker, A. R. & Jickells, T. (2010) 'Aerosol organic nitrogen over the remote Atlantic

601   Ocean'. *Atmospheric Environment*, 44 (15), pp. 1887-1893.

602

603   Mackey, K. R. M., van Dijken, G. L., Mazloom, S., Erhardt, A. M., Ryan, J., Arrigo, K. R. and Paytan, A.

604   (2010) 'Influence of atmospheric nutrients on primary productivity in a coastal upwelling

605   region', *Global Biogeochemical Cycles,* 24(4).

606

607   Mahowald, N., Jickells, T. D., Baker, A. R., Artaxo, P., Benitez-Nelson, C. R., Bergametti, G., Bond, T. C.,

608   Chen, Y., Cohen, D. D., Herut, B., Kubilay, N., Losno, R., Luo, C., Maenhaut, W., McGee, K. A., Okin, G.

609   S., Siefert, R. L. & Tsukuda, S. (2008) 'Global distribution of atmospheric phosphorus sources,

610   concentrations and deposition rates, and anthropogenic impacts'. *Global Biogeochemical Cycles*, 22

611   (4), pp. n/a-n/a.

612

613   Maier, G., Glegg, G. A., Tappin, A. D., & Worsfold, P. J. (2012). A high resolution temporal study of

614   phytoplankton bloom dynamics in the eutrophic Taw Estuary (SW England). Science of The Total

615   Environment, 434, 228-239.

616

617   Martino, M., Hamilton, D., Baker, A. R., Jickells, T. D., Bromley, T., Nojiri, Y., Quack, B. & Boyd, P. W.

618   (2014) 'Western Pacific atmospheric nutrient deposition fluxes, their impact on surface ocean

619   productivity'. *Global Biogeochemical Cycles*, 28 (7), pp. 712-728.

620

621   Moore, C. M., Mills, M. M., Arrigo, K. R., Berman-Frank, I., Bopp, L., Boyd, P. W., Galbraith, E. D., Geider,

622   R. J., Guieu, C., Jaccard, S. L., Jickells, T. D., La Roche, J., Lenton, T. M., Mahowald, N. M., Maranon, E.,

623   Marinov, I., Moore, J. K., Nakatsuka, T., Oschlies, A., Saito, M. A., Thingstad, T. F., Tsuda, A. & Ulloa, O.

624   (2013) 'Processes and patterns of oceanic nutrient limitation'. *Nature Geosci*, 6 (9), pp. 701-710.

625

626   Myriokefalitakis, S., Nenes, A., Baker, A. R., Mihalopoulos, N. & Kanakidou, M. (2016) 'Bioavailable

627   atmospheric phosphorous supply to the global ocean: a 3-D global modeling study'. *Biogeosciences*,

628   13 (24), pp. 6519-6543.

629

630   Okin, G. S., Baker, A. R., Tegen, I., Mahowald, N. M., Dentener, F. J., Duce, R. A., Galloway, J. N., Hunter,

631   K., Kanakidou, M., Kubilay, N., Prospero, J. M., Sarin, M., Surapipith, V., Uematsu, M. & Zhu, T. (2011)

632   'Impacts of atmospheric nutrient deposition on marine productivity: Roles of nitrogen, phosphorus,

633   and iron'. *Global Biogeochemical Cycles*, 25 (2), pp. n/a-n/a.

634

635   Ottley, C. J. & Harrison, R. M. (1992) 'The spatial distribution and particle size of some inorganic

636   nitrogen, sulphur and chlorine species over the North Sea'. *Atmospheric Environment. Part A. General

637   Topics*, 26 (9), pp. 1689-1699.

638

639   Owens, N. J. P., Galloway, J. N. and Duce (1992) 'Episodic atmospheric nitrogen deposition to

640   oligotrophic oceans', *Nature,* 357(6377), pp. 397-399.

641

642   Park, G.-H., Lee, S.-E., Kim, Y.-i., Kim, D., Lee, K., Kang, J., Kim, Y.-H., Kim, H., Park, S. and Kim, T.-W.

643   (2019) 'Atmospheric deposition of anthropogenic inorganic nitrogen in airborne particles and

644   precipitation in the East Sea in the northwestern Pacific Ocean', *Science of The Total Environment,* 681,

645   pp. 400-412.

646

647   Redfield, A. C. (1958) 'THE BIOLOGICAL CONTROL OF CHEMICAL FACTORS IN THE ENVIRONMENT'.

648   *American Scientist*, 46 (3), pp. 230A-221.

649

650   Rees, A. P., Hope, S. B., Widdicombe, C. E., Dixon, J. L., Woodward, E. M. S. and Fitzsimons, M. F. (2009)

651   'Alkaline phosphatase activity in the western English Channel: Elevations induced by high summertime

652   rainfall', *Estuarine, Coastal and Shelf Science,* 81(4), pp. 569-574.

653

654   Schmidt, K., Birchill, A. J., Atkinson, A., Brewin, R. J. W., Clark, J. R., Hickman, A. E., Johns, D. G., Lohan,

655   M. C., Milne, A., Pardo, S., Polimene, L., Smyth, T. J., Tarran, G. A., Widdicombe, C. E., Woodward, E.

656   M. S., & Ussher, S. J. (2020). Increasing picocyanobacteria success in shelf waters contributes to long-

657   term food web degradation. Global Change Biology, 26(10), 5574-5587.

658

659   Sharples, J., Moore, C. M., Hickman, A. E., Holligan, P. M., Tweddle, J. F., Palmer, M. R. and Simpson,

660   J. H. (2009) 'Internal tidal mixing as a control on continental margin ecosystems', *Geophysical Research*

661   *Letters,* 36(23).

662

663   Singh, A., Gandhi, N. and Ramesh, R. (2012) 'Contribution of atmospheric nitrogen deposition to new

664   production in the nitrogen limited photic zone of the northern Indian Ocean', *Journal of Geophysical*

665   *Research: Oceans,* 117(C6).

666

667   Slinn, S. A. & Slinn, W. G. N. (1980) 'Predictions for particle deposition on natural waters'. *Atmospheric*

668   *Environment (1967)*, 14 (9), pp. 1013-1016.

669

670   Spokes, L. J. & Jickells, T. D. (2005) 'Is the atmosphere really an important source of reactive nitrogen

671   to coastal waters?'. *Continental Shelf Research*, 25 (16), pp. 2022-2035.

672

673   Spokes, L. J., Yeatman, S. G., Cornell, S. E. & Jickells, T. D. (2000) 'Nitrogen deposition to the eastern

674   Atlantic Ocean. The importance of south-easterly flow'. *Tellus B*, 52 (1), pp. 37-49.

675

676   Statham, P. J. (2012) 'Nutrients in estuaries — An overview and the potential impacts of climate

677   change'. *Science of The Total Environment*, 434 pp. 213-227.

678

679   Wang, Q., Song, J., Li, X., Yuan, H., Li, N., Duan, L. and Ren, C. (2019) 'Geochemical characteristics and

680   potential biogeochemical effect of water-soluble ions in atmospheric aerosols over the western

681   boundary regions of Pacific Ocean', *Atmospheric Research,* 227, pp. 101-111.

682

683   Woodward, E. M. S., Harris, C. (2019) 'Nutrient concentration profiles from long term time series at

684   Station L4 in the Western English Channel from 2000 to 2017'. *British Oceanographic Data Centre,*

685   *National Oceanography Centre, NERC, UK*. doi:10/c2rb.

686

687   Woodward, E. M. S. and Rees, A. P. (2001) 'Nutrient distributions in an anticyclonic eddy in the

688   northeast Atlantic Ocean, with reference to nanomolar ammonium concentrations', *Deep Sea*

689   *Research Part II: Topical Studies in Oceanography,* 48(4), pp. 775-793.

690

691   Yang, M., Bell, T. G., Brown, I. J., Fishwick, J. R., Kitidis, V., Nightingale, P. D., Rees, A. P. and Smyth, T.

692   J. (2019) 'Insights from year-long measurements of air–water CH4 and CO2 exchange in a coastal

693   environment', *Biogeosciences,* 16(5), pp. 961-978.

694

695   Yang, M., Bell, T. G., Hopkins, F. E., Kitidis, V., Cazenave, P. W., Nightingale, P. D., Yelland, M. J., Pascal,

696   R. W., Prytherch, J., Brooks, I. M. & Smyth, T. J. (2016a) 'Air–sea fluxes of CO2 and CH4 from the Penlee

697   Point Atmospheric Observatory on the south-west coast of the UK'. *Atmos. Chem. Phys.*, 16 (9), pp.

698   5745-5761.

699

700   Yang, M., Bell, T. G., Hopkins, F. E. & Smyth, T. J. (2016b) 'Attribution of atmospheric sulfur dioxide

701   over the English Channel to dimethyl sulfide and changing ship emissions'. *Atmos. Chem. Phys.*, 16 (8),

702   pp. 4771-4783.

703

704   Yeatman, S. G., Spokes, L. J., Dennis, P. F. & Jickells, T. D. (2001) 'Can the study of nitrogen isotopic

705   composition in size-segregated aerosol nitrate and ammonium be used to investigate atmospheric

706   processing mechanisms?'. *Atmospheric Environment*, 35 (7), pp. 1337-1345.

707

708   Yeatman, S. G., Spokes, L. J. & Jickells, T. D. (2001) 'Comparisons of coarse-mode aerosol nitrate and

709   ammonium at two polluted coastal sites'. *Atmospheric Environment*, 35 (7), pp. 1321-1335.

710

711